ResearchGate

See discussions, stats, and author profiles for this publication at: https://www.researchgate.net/publication/260293707

Time-Resolved Studies of the Acoustic Vibrational Modes of Metal and Semiconductor Nano-objects

ARTICLE *in* JOURNAL OF PHYSICAL CHEMISTRY LETTERS · MARCH 2014

Impact Factor: 7.46 · DOI: 10.1021/jz4027248

CITATIONS
12

READS
129

4 AUTHORS, INCLUDING:

Kuai Yu
Stanford University
20 PUBLICATIONS **547** CITATIONS
SEE PROFILE

Gregory V Hartland
University of Notre Dame
148 PUBLICATIONS **6,275** CITATIONS
SEE PROFILE

Available from: Kuai Yu
Retrieved on: 30 January 2016

THE JOURNAL OF PHYSICAL CHEMISTRY Letters

Perspective

pubs.acs.org/JPCL

Time-Resolved Studies of the Acoustic Vibrational Modes of Metal and Semiconductor Nano-objects

Todd A. Major, Shun Shang Lo, Kuai Yu, and Gregory V. Hartland*

Department of Chemistry and Biochemistry, University of Notre Dame, Notre Dame, Indiana 46556-5670, United States

ABSTRACT: Over the past decade, there have been a number of transient absorption studies of the acoustic vibrational modes of metal and semiconductor nanoparticles. This Perspective provides an overview of this work. The way that the frequencies of the observed modes depend on the size and shape of the particles is described, along with their damping. Future research directions are also discussed, especially how these measurements provide information about the way nano-objects interact with their environment.

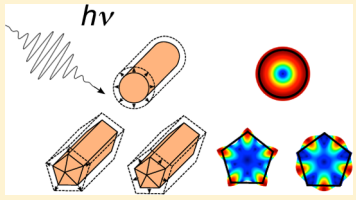

Time-resolved spectroscopy is capable of supplying detailed information about the properties of metal and semiconductor nanoparticles.[1,2] The majority of studies have been concerned with the different energy relaxation processes of the photoexcited electrons and holes.[3−5] However, these experiments can also supply information about mechanical properties. For high-quality samples, acoustic vibrations appear as oscillations in the time-resolved traces. These modes are excited by energy injection from an ultrafast pump pulse, causing periodic expansion and contraction of the nanoparticle lattice. The acoustic vibrations are detected by their coupling to the optical resonances of the nanoparticles.[6,7] The frequencies of the acoustic modes depend on the size and shape of the nano-objects and their elastic constants. Thus, time-resolved spectroscopy offers a way of measuring these constants.[6,7] The lifetimes of the oscillations measured from time-resolved experiments also provide information about how the nanoparticles interact with their environment.[8,9] The results of these experiments are relevant to the development of nanoelectromechanical systems (NEMS) for ultrasensitive charge or mass sensing.[10−12]

Coherent acoustic vibrations in metal and semiconductor nanoparticles can be generated by ultrafast laser excitation and give unique information about the mechanical properties of the particles.

Acoustic vibrations have been studied for many nanoparticle samples with different sizes, shapes, and compositions.[13,14] Analytical continuum mechanics expressions are available for several cases, such as the radially symmetric modes of spheres and rods and the extensional modes for rods and bipyramids.[15−18] For more complicated shapes, finite elemental analysis is often used to predict the frequencies of the acoustic vibrations. In most cases, the calculated frequencies match the experimental values.[14] Thus, the way that the vibrational frequencies depend on the size and shape of the nanostructure is well-understood. However, the lifetimes of the acoustic vibrations are more complex and more difficult to study. Ensemble measurements typically do not give good information about the lifetime due to sample inhomogeneity (particles with different sizes and shapes have different periods, which washes out lifetime information).[19,20] Exceptions to this include the monodisperse gold bipyramids examined in refs 9, 17, and 18 and systems where the environmental damping is very strong.[21] The recent development of single-particle transient absorption techniques has allowed lifetime measurements to be made for a variety of different nanostructures.[22−24] Because of the small signal levels in these experiments, the size of the particles is limited to several tens of nanometers. However, it may be possible to study smaller nanoparticles by using antenna effects to reduce the excitation volume.[25]

This Perspective will review recent progress in the studies of the acoustic vibrations of metal and semiconductor nanostructures using time-resolved spectroscopy. The excitation mechanism will be briefly discussed for both metal and semiconductor nanomaterials. Examples will then be given for calculations of the vibrational frequencies using analytic continuum mechanics expressions for spheres and rods and finite element analysis for more complicated shapes. Finally, the lifetimes of the acoustic vibrational modes will also be discussed, in particular, the way that they are affected by the environment.

For metals, the major process for generating acoustic vibrations is impulsive heating.[6,7,18,19] Ultrafast excitation by the pump pulse heats the electrons in the conduction band, creating a large temperature difference between the electrons and lattice. Energy is then transferred from the electrons to the lattice through electron−phonon coupling over a several picosecond time scale.[6,7,14] This fast heating process impulsively excites the lattice vibrations of the nanoparticle that correlate with the expansion coordinate. These modes are

Received: December 18, 2013
Accepted: February 12, 2014

 © XXXX American Chemical Society dx.doi.org/10.1021/jz4027248 | J. Phys. Chem. Lett. 2014, 5, 866−874

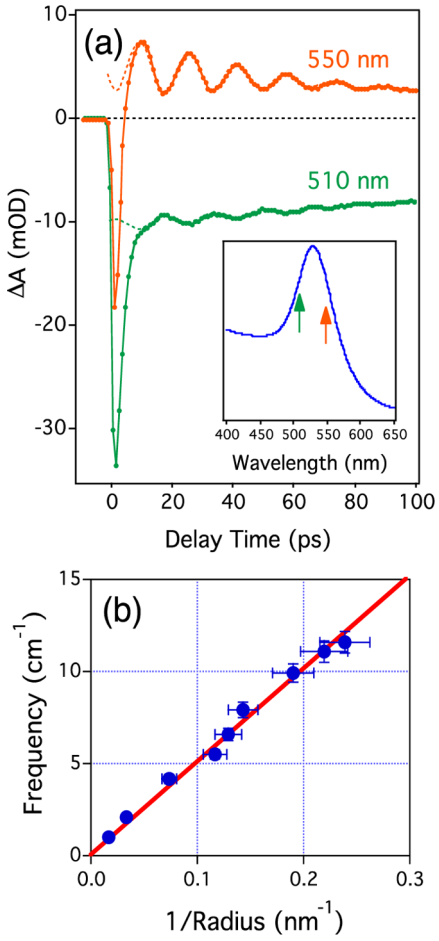

Figure 1. (a) Transient absorption traces for 48 ± 5 nm diameter Au nanospheres recorded with 510 and 550 nm probe pulses. The inset shows the absorption spectrum of the Au nanopshere sample, and the colored arrows correspond to the probe wavelengths relative to the plasmon resonance of the nanospheres. (b) Frequency of the acoustic vibrations of Au nanopspheres as a function of $1/R$. The line shows the calculated frequency for the breathing mode. Reproduced from ref 14 with permission.

detected in transient absorption measurements because they produce a change in size of the particle, which shifts the position of the plasmon resonance.[26] Figure 1a shows transient absorption traces for 48 ± 5 nm Au nanoparticles in water recorded at wavelengths of 550 and 510 nm, which correspond to opposite sides of the plasmon band.[26] The modulations are 180° out-of-phase for the two traces, which confirms that the signal arises from a shift in the position of the plasmon resonance.[26] Analysis of the phase of the modulations shows that lattice heating via electron−phonon coupling is the major driving force for generating the vibrations; for these particles, effects such as hot electron pressure play a minor role.[26−28]

There are fewer reports on the acoustic vibrations of semiconductor nanomaterials in the literature than those for metals. In general, coherent acoustic vibrations for semiconductor nanomaterials are generated through a displacive excitation mechanism; promotion of electrons to the conduction band by ultrafast excitation changes the unit cell size, which launches acoustic phonons of the nano-object.[29] Modes that cause a significant change in volume can create a transient absorption signal through deformation potential coupling,[29] although other excitation and coupling mechanisms have been proposed.[30]

The earliest studies of acoustic vibrations using time-resolved spectroscopy were for spherical semiconductor[31] and metal[32−34] nanoparticles. For nanospheres, the radially symmetric modes, often called the "breathing" modes, are typically excited in time-resolved measurements. These modes are well-known; a continuum mechanical expression for the breathing modes of spheres was first derived by Lamb in 1882.[15] For a sphere in a homogeneous medium, the equations that describe the displacement and stress for the radially symmetric modes are[15,35]

$$\begin{cases} \dfrac{d^2u_i}{dr^2} + \dfrac{2}{r}\dfrac{du_i}{dr} + \left(k_i^2 - \dfrac{2}{r^2}\right)u_i = 0 \\ \sigma_{rr}^i(r) = (\lambda_i + 2\mu_i)\dfrac{du_i}{dr} + 2\lambda_i\dfrac{u_i}{r} \end{cases} \quad (1)$$

where u_i and σ_{rr}^i are the displacement and radial stress in the particle (i = p) or the surrounding medium (i = m), λ_i and μ_i are the Lamé constants for the particle or the medium, $k_i = \omega/c_l^i$, and c_l^i is the longitudinal speed of sound in medium i.[15,35] The general solutions to this equation are displacements in the particle and medium of $u_p = j_1(k_p r)$ and $u_m = Ah_1^{(2)}(k_m r)$, where A is a constant and j_1 and $h_1^{(2)}$ are spherical Bessel and Hankel functions. This choice of functions is dictated by the constraints that the displacement must be finite inside of the sphere and correspond to an outgoing wave in the medium. The boundary conditions are continuity of the displacement and radial stress at the surface of the sphere ($r = a$). Applying these conditions gives an eigenvalue equation that has a complex solution, the real part of which gives the vibrational frequency and the imaginary part of which gives the damping.[35]

For a free sphere, the boundary conditions are that the radial stress at the surface is zero, that is, $\sigma_{rr}^s(a) = (\lambda_p + 2\mu_p)(du_p/dx)_{r=a} + 2\lambda_p(u_p(a)/a) = 0$. This case is much simpler to solve and yields the following eigenvalue equation

$$\tau j_0(\tau) = \frac{4\mu_p}{\lambda_p + 2\mu_p} j_1(\tau) = \frac{2(1-2\nu_p)}{1-\nu_p} j_1(\tau) \quad (2)$$

where $\tau = k_p a$. This equation can be written in the more familiar form of $\tau\cot(\tau) = 1 - (\tau c_l/2c_t)^2$.[15,35] Solving eq 2 gives values for τ and, therefore, the vibrational frequency $\omega = \tau c_l/a$. Figure 1b shows a plot of the frequency of the acoustic mode (determined by fitting the transient absorption data to a damped cosine term) versus $1/R$ for gold nanoparticle samples with different average sizes.[36] The line in Figure 1b gives the calculated frequency of the fundamental breathing mode for a free sphere determined using the speeds of sound for bulk gold. The calculations are in excellent agreement with the data, which shows that the environment does not significantly affect the frequencies.[36]

The data in Figure 1b show that the elastic constants of 8 nm diameter nanoparticles are the same as those for the bulk metal. A significant issue is determining the size at which this is no longer true, that is, the point where the elastic properties of the particles become size-dependent. Figure 2 shows the results of experiments for small Pt and Au nanoparticles made by low-energy cluster beam deposition.[37,38] The data has a linear relationship between size and period, which matches the predictions of eq 2 quite well.[37,38] Such small clusters are typically faceted, not spherical. To account for this, the authors also calculated the breathing mode frequencies for truncated octahedral, decahedral, and icosahedral particles using atomistic

dx.doi.org/10.1021/jz4027248 | J. Phys. Chem. Lett. 2014, 5, 866−874

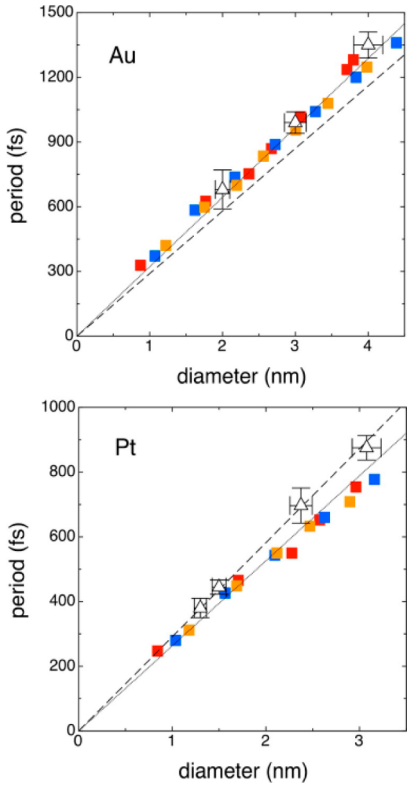

Figure 2. Period versus diameter for Au (top) and Pt (bottom) nanoparticles. Open triangles represent experimental data; the red, yellow, and blue symbols show calculations for faceted nanoparticles with truncated octahedral, decahedral, and icosahedral shapes.[38] The dashed and solid lines were calculated using continuum elastic theory for either free particles or particles in a solid matrix. Reproduced from ref 38 with permission.

simulations.[38] The calculated values are also in good agreement with the data.

These results show that the elastic constants of small nanoparticles prepared by low-energy cluster beam deposition are the same as those for the bulk materials, down to sizes less than 100 atoms for Pt, and that the details of the shape are not particularly important.[37,38] However, other reports on Au clusters found different results.[39−41] Specifically, Varnavski et al. observed a single size-independent mode for 1.1−2.2 nm Au clusters with a period of 450 fs (2.2 THz).[39] Studies on neutral and charged monolayer-protected $Au_{25}L_{18}$ clusters also show a vibrational mode with a similar frequency at 2.4 THz.[40,41] This mode is attributed to the vibration of the 13 atom Au core modified by the additional mass from the outer ligands. Quantum-confined semiconductors were also found to show deviations from theory at small sizes,[42,43] which was attributed to effects from the nanoparticle surface.

For nanorods, two different vibrational modes are excited by impulsive heating, the fundamental extensional mode and the radial breathing modes.[16] This is very clearly seen in the transient absorption traces for a single gold nanorod presented in Figure 3.[44] The higher-frequency mode is assigned to the breathing mode, and the lower-frequency mode is the extensional mode. Analytic continuum mechanics expressions are available for both of these modes. The extensional mode has been well-studied, and the vibrational frequencies are given by[45,46]

$$\omega_{\text{ext}} = \frac{(2n+1)}{L}\pi\sqrt{\frac{E}{\rho}} \tag{3}$$

where L is the length of the rod, E is Young's modulus, and ρ is the density. A closed form expression can also be derived for the breathing mode in the limit of an infinite cylinder. In this case, the equations that describe the displacement and radial stress are[46]

$$\begin{cases} \dfrac{d^2u_i}{dr^2} + \dfrac{1}{r}\dfrac{du_i}{dr} + \left(k_i^2 - \dfrac{1}{r^2}\right)u_i = 0 \\ \sigma_{rr}^i(r) = (\lambda_i + 2\mu_i)\dfrac{du_i}{dr} + \lambda_i\dfrac{u_i}{r} \end{cases} \tag{4}$$

The general solutions for the displacement in the cylinder (which is now the "particle") and the medium are now $u_p = J_1(k_p r)$ and $u_m = H_1^{(2)}(k_m r)$, respectively, where J_1 and $H_1^{(2)}$ are Bessel functions of the first kind and Hankel functions,

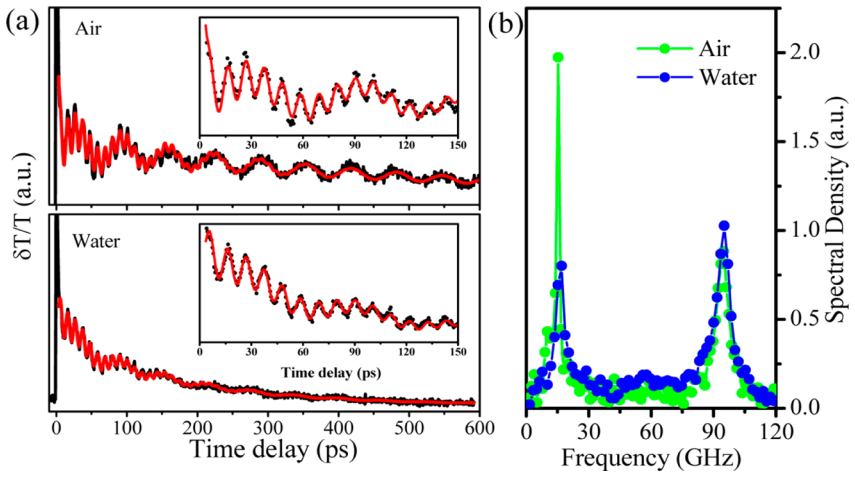

Figure 3. (a) Transient absorption trace of a supported nanorod in air (top left) and in water (bottom left). The higher-frequency (~90 GHz) and lower-frequency (~15 GHz) modes correspond to the breathing and extensional mode of the nanorod, respectively. (b) Fourier transform of the traces in (a). The contribution of the extensional mode of the nanorod to the dynamics is shown to be greatly damped due to the presence of lubrication forces.[44] Reproduced from ref 44 with permission.

dx.doi.org/10.1021/jz4027248 | J. Phys. Chem. Lett. 2014, 5, 866−874

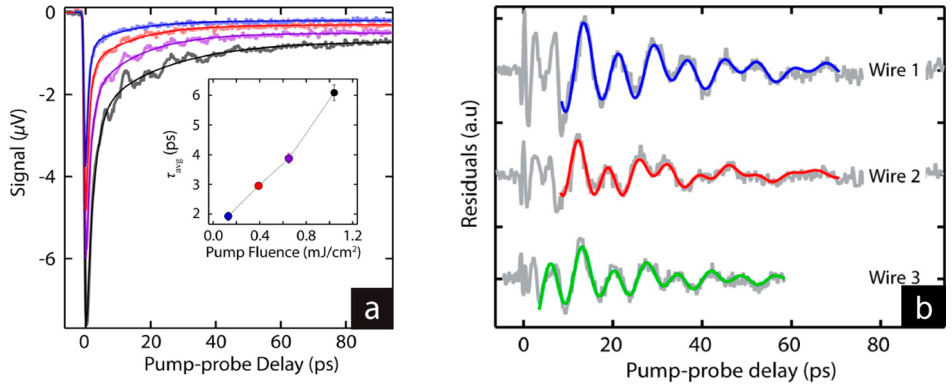

Figure 4. (a) Transient absorption traces for a single CdTe nanowire at varying pump fluences. The inset shows the average value of the fast decay component as a function of pump fluence. (b) Residuals from three CdTe nanowire traces (in gray) fit to a damped double cosine function. The residuals show a complex beating pattern, which is attributed to a combination of the fundamental and first overtone breathing modes. Reproduced from ref 59 with permission.

respectively. The boundary conditions are, again, continuity of the displacement and stress at the surface of the cylinder.

As was the case for the breathing modes of a sphere, the boundary conditions for a free cylinder are much simpler than that for a cylinder embedded in a medium. For a free cylinder with radius a, the radial stress at the surface is zero, $\sigma_{rr}^{c}(a) = 0$, which yields the eigenvalue equation

$$\tau J_0(\tau) = \frac{(1 - 2\nu_p)}{1 - \nu_p} J_1(\tau) \tag{5}$$

where $\tau = k_p a$, and ν_p is Poisson's ratio for the cylinder. Although eqs 4 and 5 correspond to the limit of an infinite cylinder, finite element calculations have shown that the results are accurate for the breathing modes of nanorods for aspect ratios (L/R) greater than ~3.[47] The frequencies predicted by eqs 3 and 4 are in good agreement with single-particle experimental data[44,48] (ensemble measurements typically do not give reliable values for nanorods due to problems with the size distribution).

There have been a number of experimental studies of the acoustic modes of metal nanorods[16,48−54] and nanowires.[55−59] One major result of the studies on Au nanorods was to demonstrate how the crystal structure affects the vibrational response. Nanorods grown by solution-phase techniques are typically single crystals, with different crystal structures depending on how they are synthesized.[60] For the extensional mode, the value of Young's modulus corresponding to the growth direction of the nanorods must be used in eq 3; nanorods with a [110] growth direction show different extensional mode frequencies compared to rods with a [100] growth direction.[50,51] However, the details of the crystal structure do not appear to affect the breathing mode; good agreement is found between the measured and calculated periods using isotropic elastic constant data.[44,48] This may be because the breathing mode averages over many different crystal directions.

Breathing vibrational modes have also been observed for CdTe nanowires. Figure 4 shows transient absorption traces for several single nanowires recorded using transient absorption microscopy.[59] Figure 4a shows power-dependent results for a single nanowire, where the acoustic vibrations can be clearly seen at high powers, and Figure 4b shows data for several nanowires, after subtraction of the background signal. A complicated beating pattern is observed, which is attributed to contributions to the signal from both the fundamental breathing mode and the first overtone. The lines in the figure are fits to the data using two cosine terms for the fundamental and overtone modes. These results are somewhat different than those for metal nanowires, where usually the fundamental mode dominates the transient absorption traces.[56,61] It is not clear why the overtone mode contributes so strongly to the vibrational response of the CdTe nanowires. This may be due to the details of the probe transition, which is not well-understood for these materials.[59]

The acoustic vibrations of a large number of different shapes have been studied, including spherical core−shell particles of different types (bimetallics,[62−64] metal/dielectrics,[65,66] and hollow particles[67,68]), nanotriangles,[28,69] nanocubes,[70] nanocages,[71] dumbbells,[72] bipyramids,[9,17,18] nanorings,[22,73] and nanoplates.[74,75] Similarly to spheres, analytical calculations have been derived for the breathing mode of spherical core−shell nanoparticles,[63,76] and they match well with experimental results, given that the thicknesses of the core and the shell are both known. However, continuum mechanical expressions do not exist for all of the other nanoparticle shapes, and finite element calculations are often needed to determine the form of the vibrational modes and their frequencies. The different shapes that have been analyzed by finite element methods include nanorods,[47] nanotriangles,[28] nanocubes,[70] nanoboxes,[71] dumbbells,[72] nanobipyramids,[9] nanorings,[22] and faceted nanowires.[24] In these calculations, typically the frequencies and mode shapes for all of the vibrational modes of the nano-object are determined up to a certain frequency. A prediction of the relative contributions of the different modes to the transient absorption signal is then made by projecting the mode shape onto the shape of the nano-object.[16,76]

An example of finite element analysis for hollow Au−Ag nanoboxes is shown in Figure 5.[71] The analysis predicts that two breathing modes should occur, and the form of these two modes is shown in Figure 5a for nanoboxes with different edge length (L) to wall thickness (w) ratios. The calculated reduced frequencies $\bar{\omega} = \omega L/(E/\rho)^{1/2}$ are plotted against L/w in Figure 5b, along with experimental data for different samples. The size of the symbols for the calculations represents the expected relative contribution of the mode to the transient absorption experiments. The calculations predict that the low-frequency mode should dominate the response at small values of L/w, and the high-frequency mode should dominate at large L/w values. The experimental results confirm this prediction, and the

dx.doi.org/10.1021/jz4027248 | J. Phys. Chem. Lett. 2014, 5, 866−874

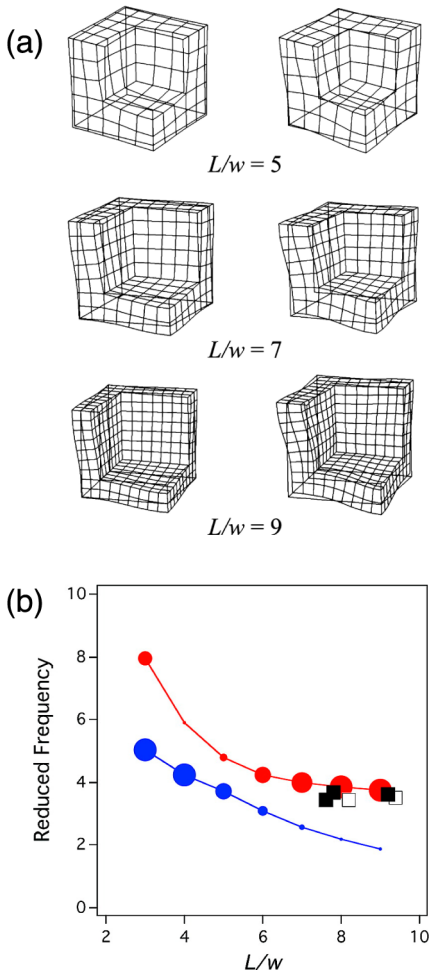

Figure 5. (a) Shapes of the vibrational modes for nanoboxes with varying length/width (L/w). Only one eighth of the nanobox is shown to better illustrate the vibration. (b) Calculated and measured reduced frequencies for Au−Ag nanoboxes as a function of L/w. The circle size represents the relative contribution of the mode to the transient absorption signal. The squares represent the measured reduced frequencies (the error bar is contained within the symbol). Reproduced from ref 71 with permission.

measured frequencies are in excellent agreement with the calculated results.

Another example of the use of finite element analysis for assigning vibrational modes in nanostructures is presented in Figure 6.[24] Figure 6a shows transient absorption traces for a single suspended Au nanowire, where two modes with similar frequencies can be clearly seen for the trace recorded in air. The periods are close to that expected for the breathing mode of the nanowire. Because solution-grown Au nanowires are known to have pentagonal cross sections,[77] finite element calculations were performed for nanowires with different shapes. The calculations show that faceted pentagonal nanowires have two breathing modes that correspond to motions at the apexes or faces of the structure. Figure 6b shows the form of these modes for structures with different values of the radius of curvature at the apexes; $r/r_c = 0$ corresponds to sharp apexes (perfect pentagonal cross section), and $r/r_c = 1$ corresponds to a circular cylinder. The scaled frequencies and expected contribution of the two modes to the transient absorption signal are presented in Figure 6c. For a circular cylinder, only the breathing mode is expected to contribute to the transient absorption signal.

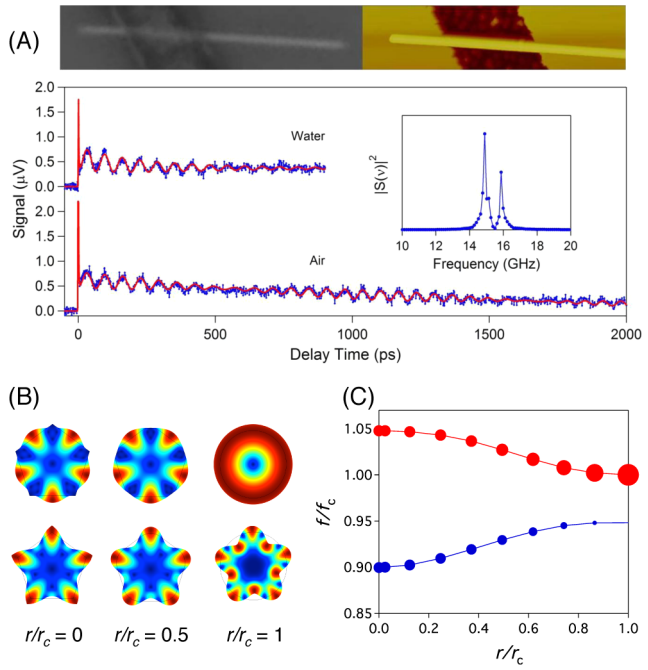

Figure 6. (a) Transient absorption trace for a suspended Au nanowire; the inset shows a Fourier transform of the data. Scattered light (left) and AFM (right) images of the nanowire are shown in the top panel. The diameter of the nanowire measured by AFM is 159 ± 5 nm. (b) Mode shapes for pentagonal nanowires as a function of the radius-of-curvature at the apexes; $r/r_c = 0$ corresponds to a sharp pentagonal cross section, and $r/r_c = 1$ corresponds to a circular cross section. (c) Normalized frequency (f/f_c) versus relative radius-of-curvature (r/r_c). The size of the circles represents the contribution of the mode to the transient absorption signal. Reproduced from ref 24 with permission.

Breaking the symmetry mixes the breathing mode with a five-fold-symmetric "whispering gallery" mode to produce two breathing modes, whose frequencies and amplitudes depend on the radius of curvature at the apexes of the structure. Note that the whispering gallery modes do not contribute to the transient absorption signal for the circular cylinder. Values of the radius of curvature of $r/r_c \approx 0.5$ provide reasonable agreement with the experimental data (similar intensities in the transient absorption traces and frequency differences for the two modes on the order of 10%). Complex beating patterns have also been observed for suspended Cu nanowires; however, in this case, the signal was attributed to two nanowires in close contact.[78]

The lifetimes of the vibrational modes of metal and semiconductor nanoparticles is also an active research topic as this quantity provides detailed information about how the nanostructures interact with their environment.

The lifetimes of the vibrational modes of metal and semiconductor nanoparticles is also an active research topic as this quantity provides detailed information about how the nanostructures interact with their environment. A number of different studies have appeared in the past several years that

dx.doi.org/10.1021/jz4027248 | J. Phys. Chem. Lett. 2014, 5, 866−874

have focused on understanding how the local environment affects the vibrational damping.[9,17−19,22,23,44,48,61,74,75,79,80] Recent measurements have also explored effects from anelastic processes in the material of the nano-object and surface-bound ligands.[9,23]

Discussions of the vibrational damping of nano-objects are best done through the quality factors, $Q = \omega/2\gamma$, where ω is the frequency and γ is the damping constant. This removes the trivial size dependence of the results (both the frequency and damping constant scale with size in the same way). In general, the quality factor can be separated into contributions from intrinsic effects Q_{int}, such as anelastic processes, and effects from the environment Q_{env}[9,17]

$$\frac{1}{Q} = \frac{1}{Q_{int}} + \frac{1}{Q_{env}} \tag{6}$$

The contribution from the environment can be calculated from continuum mechanics for spheres and rods by imposing the boundary conditions that the displacement and stress are continuous at the interface. Applying these boundary conditions yields the following eigenvalue equations for a sphere (eq 7a) and a rod (eq 7b)[24]

$$(\lambda_p + 2\mu_p)\tau\frac{j_0(\tau)}{j_1(\tau)} - 4\mu_p = (\lambda_m + 2\mu_m)(\tau/\alpha)\frac{h_0^{(2)}(\tau/\alpha)}{h_1^{(2)}(\tau/\alpha)} - 4\mu_m \tag{7a}$$

$$(\lambda_p + 2\mu_p)\tau\frac{J_0(\tau)}{J_1(\tau)} - 2\mu_p = (\lambda_m + 2\mu_m)(\tau/\alpha)\frac{H_0^{(2)}(\tau/\alpha)}{H_1^{(2)}(\tau/\alpha)} - 2\mu_m \tag{7b}$$

where λ_i and μ_i are the Lamé constants for the particle and the medium, $\tau = k_p a$, and $\alpha = k_p/k_m$. The solutions for τ obtained from these equations are complex and give complex frequencies $\omega = \tau c_l^p/a$. The real part of ω corresponds to the vibrational frequency, and the imaginary part corresponds to the damping constant. Note that the quality factor $Q = \mathrm{Re}(\tau)/2\,\mathrm{Im}(\tau)$ can be directly calculated from the solutions.

For particles in a solid medium, eqs 7a and 7b show that the medium has very little effect on the vibrational frequency (see Figure 2). However, the damping strongly depends on the difference in acoustic impedance ($Z = \rho c_l$) between the particle and the medium. Small values of ΔZ give strong damping (sound waves easily radiate from the particle out into the medium), whereas for large values of ΔZ, the sound waves are reflected at the interface, so that the acoustic energy is contained within the particle for longer times.[21] For particles in a liquid, the viscosity of the liquid must be incorporated into the calculations.[9,17,18,23,59,81] For the breathing modes (eqs 7a and 7b), the effects of viscosity can be included by adding frequency-dependent imaginary terms to the speeds of sound for the medium, $c_t^m \rightarrow ((c_l^m)^2 + i\omega(\lambda' + 2\mu')/\rho)^{1/2}$ and $c_t^m \rightarrow (i\omega\mu'/\rho)^{1/2}$, where λ' and μ' are the second viscosity coefficient and the shear viscosity of the liquid, respectively.[81] The analysis is more complicated for vibrations that involve the extensional motion and requires details about the shape of the particles.[18] It is important to note that this analysis is only appropriate for particles in a homogeneous medium; it does not apply to particles supported on a substrate, which is the typical way of doing single-particle measurements, for example.

Experimental studies of viscous damping of the vibrational modes of nanoparticles in a liquid were first done by Pelton et al. using ensemble transient absorption measurements.[9,17] These measurements were done on Au bipyramids, which have very narrow size distributions.[82] In their initial work, Q_{env} was calculated by modeling the bipyramids as a rod vibrating in a viscous fluid. The total quality factor Q was measured, and Q_{int} was determined as a fit parameter through eq 6. More recently, these workers have examined the damping of these materials in a series of water−glycerol mixture.[18] The results show that non-Newtonian viscoelastic effects in the fluid are important in these systems.[18]

The samples used by Pelton and co-workers were unusual in that their size distributions were narrow enough to allow meaningful measurements of the damping times. This is not typical, and for most systems, single-particle measurements are needed.[19,83] The first single-particle measurements in a homogeneous liquid environment were performed by the Orrit group.[23] In these experiments, single Au nanoparticles (rods and spheres) were optically trapped, and the vibrational response was measured by transient absorption microscopy. The contribution from fluid damping was calculated assuming a homogeneous environment,[81] and Q_{int} was determined from eq 6. The authors found large differences between the two samples; for the spheres, $\langle Q_{int}\rangle = 40$, and for the nanorods, $\langle Q_{int}\rangle = 84$. This is most likely due to the differences in crystal structure; the nanorods are single crystals, whereas the spheres are polycrystalline, and polycrystalline materials are expected to show stronger aneleastic effects.[23] Differences were also observed between particles of the same type; the standard deviations for the measurements were on the order of 30−40%. This was attributed to differences in the structure of the individual particles.

Both studies discussed above measured a total quality factor and then made an assumption about either the fluid damping or intrinsic contributions to analyze the results. We have used a different approach to determine the intrinsic and fluid damping for metal nanostructures. In our experiments, single Au nanowires with lengths of approximately 10 μm are suspended over trenches, and transient absorption traces are recorded in air and liquid environments.[24] Using eq 6 and assuming that the air results accurately give the intrinsic damping, these measurements allow us to experimentally determine both the fluid and intrinsic contributions. Figure 7 shows optical and AFM images of a suspended Au nanowire, along with transient absorption traces of the nanowire in air and water environments. The modulations clearly have a much longer lifetime for the nanowire in air compared to that in water. For this particular nanowire, $Q_{int} = 109.2 \pm 6.2$, and $Q_{fluid} = 33.1 \pm 1.5$. We were able to perform measurements on a handful of nanowires and found $\langle Q_{int}\rangle = 90 \pm 29$ and $\langle Q_{fluid}\rangle = 39 \pm 15$ (the error equals the standard deviation). The results for Q_{int} are consistent with the Orrit group measurements for nanorods, both in terms of the magnitude and the variation between particles.[23,24] This is not surprising as the nanowires are also single crystals. The average value of Q_{fluid} was also consistent with the value calculated using eq 7b of $Q_{fluid} = 43$. The calculations show that viscosity only has a minor effect on the damping and that the major effect is radiation of sound waves into the fluid. This is because the acoustic modes for these nanowires have relatively low frequencies.[24]

dx.doi.org/10.1021/jz4027248 | J. Phys. Chem. Lett. 2014, 5, 866−874

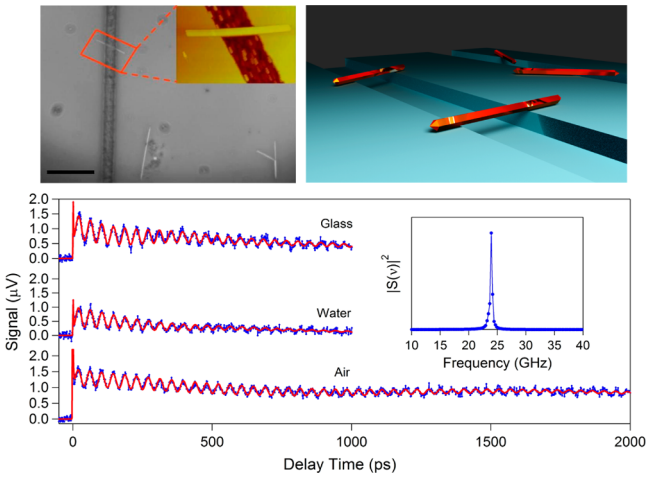

Figure 7. (Top left) Scattered light image of a single suspended gold nanowire. The scale bar represents 2 μm. The inset shows a 5 × 8 μm AFM image of the suspended wire. (Top right) Cartoon depiction of suspended gold nanowires. (Bottom) Transient absorption traces for a gold nanowire on glass (top trace), and suspended over a trench in water (middle trace) and over a trench in air (bottom trace). The inset shows the Fourier transform of the trace in air. A single peak at 24 GHz is observed, which corresponds to the breathing mode of the nanowire. Reproduced from ref 24 with permission.

Coherent acoustic vibrations in metal and semiconductor nanoparticles can be generated by ultrafast laser excitation and give unique information about the mechanical properties of the particles. The measurements show that, in general, the elastic constants of nanoparticles match known bulk values, even for particles with sizes on the order of several nanometers. Over the past several years, significant headway has also been made in understanding the damping mechanisms for the acoustic vibrations. For particles in a homogeneous environment, the breathing mode damping is reasonably well understood; the damping is typically dominated by radiation of sound waves into the medium, which is controlled by the difference in acoustic impedance between the particle and the medium. For viscous solvents, non-Newtownian viscoelastic effects can occur,[18] but more work is needed here to understand how these effects depend on the form of the vibrational motion and the properties of the liquid.

The damping rates for particles in inhomogeneous environments are less well understood. For example, a recent study of Au nanorods supported on a substrate showed an additional damping mechanism for the extensional mode that was attributed to a lubrication force between the nanorod and the substrate.[44] Other areas where more research is needed are studies of coupled systems and investigations of how the intrinsic damping of the nanoparticles depends on their crystal structure and the frequency of the acoustic modes. We expect that single-particle transient absorption measurements will become an increasingly important tool for investigating these effects.[8,14]

AUTHOR INFORMATION

Corresponding Author

*E-mail: ghartlan@nd.edu.

Notes

The authors declare no competing financial interest.

Biographies

Todd Major is a graduate student in Dr. Gregory Hartland's lab at the University of Notre Dame. Todd got his B.S. in Chemistry from Grand Valley State University in May of 2010. His research interests are in nanofabrication and instrument design.

Shun Shang Lo earned a Ph.D. in physical chemistry from the University of Toronto in 2011. That same year, he joined the Hartland Lab at the University of Notre Dame as a postdoctoral research associate. His research focuses on understanding energy/charge transfer and transport processes in nanoscale systems.

Kuai Yu obtained his Ph.D. degree from the National University of Singapore in 2013. He is currently a postdoctoral researcher in Professor Hartland's group, and his research interests focus on plasmon propagation and coupling in metal nanostructures.

Greg Hartland has worked at the University of Notre Dame since 1994, where he is currently a Full Professor. His research interests are using optical techniques to study the spectroscopy and dynamics of single nanoparticles.

ACKNOWLEDGMENTS

This work was supported by the National Science Foundation (CHE-1110560), the Office of Naval Research (Award No. N00014-12-1-1030), and the University of Notre Dame Strategic Research Initiative. The authors are extremely grateful to their collaborators, especially Aurélien Crut from the LASIM group at the Université Lyon 1 and John Sader at the University of Melbourne, for their help in understanding continuum mechanics.

REFERENCES

(1) Klimov, V. I. Optical Nonlinearities and Ultrafast Carrier Dynamics in Semiconductor Nanocrystals. *J. Phys. Chem. B* **2000**, *104*, 6112−6123.

(2) Kambhampati, P. Unraveling the the Structure and Dynamics of Excitons in Semiconductor Quantum Dots. *Acc. Chem. Res.* **2011**, *44*, 1−13.

(3) Burda, C.; Link, S.; Mohamed, M.; El-Sayed, M. The Relaxation Pathways of CdSe Nanoparticles Monitored with Femtosecond Time-Resolution from the Visible to the IR: Assignment of the Transient Features by Carrier Quenching. *J. Phys. Chem. B* **2001**, *105*, 12286−12292.

(4) Guyot-Sionnest, P.; Wehrenberg, B.; Yu, D. Intraband Relaxation in CdSe Nanocrystals and the Strong Influence of the Surface Ligands. *J. Chem. Phys.* **2005**, *123*, 074709.

(5) Knowles, K. E.; McArthur, E. A.; Weiss, E. A. A Multi-Timescale Map of Radiative and Nonradiative Decay Pathways for Excitons in CdSe Quantum Dots. *ACS Nano* **2011**, *5*, 2026−2035.

(6) Hodak, J. H.; Henglein, A.; Hartland, G. V. Photophysics of Nanometer Sized Metal Particles: Electron−Phonon Coupling and Coherent Excitation of Breathing Vibrational Modes. *J. Phys. Chem. B* **2000**, *104*, 9954−9965.

(7) Voisin, C.; Del Fatti, N.; Christofilos, D.; Vallée, F. Ultrafast Electron Dynamics and Optical Nonlinearities in Metal Nanoparticles. *J. Phys. Chem. B* **2001**, *105*, 2264−2280.

(8) Zijlstra, P.; Orrit, M. Single Metal Nanoparticles: Optical Detection, Spectroscopy and Applications. *Rep. Prog. Phys.* **2011**, *74*, 1−55.

(9) Pelton, M.; Sader, J. E.; Burgin, J.; Liu, M. Z.; Guyot-Sionnest, P.; Gosztola, D. Damping of Acoustic Vibrations in Gold Nanoparticles. *Nat. Nanotechnol.* **2009**, *4*, 492−495.

(10) Craighead, H. G. Nanoelectromechanical Systems. *Science* **2000**, *290*, 1532−1535.

(11) Li, M.; Tang, H. X.; Roukes, M. L. Ultra-Sensitive NEMS-Based Cantilevers for Sensing, Scanned Probe and Very High-Frequency Applications. *Nat. Nanotechnol.* **2007**, *2*, 114−120.
(12) Unterreithmeier, Q. P.; Faust, T.; Kotthaus, J. P. Damping of Nanomechanical Resonators. *Phys. Rev. Lett.* **2010**, *105*, 027205.
(13) Tchebotareva, A. L.; Ruijgrok, P. V; Zijlstra, P.; Orrit, M. Probing the Acoustic Vibrations of Single Metal Nanoparticles by Ultrashort Laser Pulses. *Laser Photon. Rev.* **2010**, *4*, 581−597.
(14) Hartland, G. V. Optical Studies of Dynamics in Noble Metal Nanostructures. *Chem. Rev.* **2011**, *111*, 3858−3887.
(15) Lamb, H. On the Vibrations of an Elastic Sphere. *Proc. London Math. Soc.* **1882**, *13*, 189−212.
(16) Hu, M.; Wang, X.; Hartland, G. V; Mulvaney, P.; Juste, J. P.; Sader, J. E. Vibrational Response of Nanorods to Ultrafast Laser Induced Heating: Theoretical and Experimental Analysis. *J. Am. Chem. Soc.* **2003**, *125*, 14925−14933.
(17) Pelton, M.; Wang, Y. L.; Gosztola, D.; Sader, J. E. Mechanical Damping of Longitudinal Acoustic Oscillations of Metal Nanoparticles in Solution. *J. Phys. Chem. C* **2011**, *115*, 23732−23740.
(18) Pelton, M.; Chakraborty, D.; Malachosky, E.; Guyot-Sionnest, P.; Sader, J. E. Viscoelastic Flows in Simple Liquids Generated by Vibrating Nanostructures. *Phys. Rev. Lett.* **2013**, *111*, 244502.
(19) Van Dijk, M. A.; Lippitz, M.; Orrit, M. Detection of Acoustic Oscillations of Single Gold Nanospheres by Time-Resolved Interferometry. *Phys. Rev. Lett.* **2005**, *95*, 267406.
(20) Muskens, O. L.; Del Fatti, N.; Vallée, F. Femtosecond Response of a Single Metal Nanoparticle. *Nano Lett.* **2006**, *6*, 552−556.
(21) Voisin, C.; Del Fatti, N.; Christofilos, D.; Vallée, F. Time-Resolved Investigation of the Vibrational Dynamics of Metal Nanoparticles. *Appl. Surf. Sci.* **2000**, *164*, 131−139.
(22) Marty, R.; Arbouet, A.; Girard, C.; Mlayah, A.; Paillard, V.; Lin, V. K.; Teo, S. L.; Tripathy, S. Damping of the Acoustic Vibrations of Individual Gold Nanoparticles. *Nano Lett.* **2011**, *11*, 3301−3306.
(23) Ruijgrok, P. V; Zijlstra, P.; Tchebotareva, A. L.; Orrit, M. Damping of Acoustic Vibrations of Single Gold Nanoparticles Optically Trapped in Water. *Nano Lett.* **2012**, *12*, 1063−1069.
(24) Major, T. A.; Crut, A.; Gao, B.; Lo, S. S.; Del Fatti, N.; Vallée, F.; Hartland, G. V. Damping of the Acoustic Vibrations of a Suspended Gold Nanowire in Air and Water Environments. *Phys. Chem. Chem. Phys.* **2013**, *15*, 4169−4176.
(25) Schumacher, T.; Kratzer, K.; Molnar, D.; Hentschel, M.; Giessen, H.; Lippitz, M. Nanoantenna-Enhanced Ultrafast Nonlinear Spectroscopy of a Single Gold Nanoparticle. *Nat. Commun.* **2011**, *2*, 333−337.
(26) Hartland, G. V. Coherent Vibrational Motion in Metal Particles: Determination of the Vibrational Amplitude and Excitation Mechanism. *J. Chem. Phys.* **2002**, *116*, 8048−8055.
(27) Perner, M.; Gresillon, S.; März, J.; von Plessen, G.; Feldmann, J.; Porstendorfer, J.; Berg, K. J.; Berg, G. Observation of Hot-Electron Pressure in the Vibration Dynamics of Metal Nanoparticles. *Phys. Rev. Lett.* **2000**, *85*, 792−795.
(28) Bonacina, L.; Callegari, A.; Bonati, C.; van Mourik, F.; Chergui, M. Time-Resolved Photodynamics of Triangular-Shaped Silver Nanoplates. *Nano Lett.* **2006**, *6*, 7−10.
(29) Zeiger, H. J.; Vidal, J.; Cheng, T. K.; Ippen, E. P.; Dresselhaus, G.; Dresselhaus, M. S. Theory for Displacive Excitation of Coherent Phonons. *Phys. Rev. B* **1992**, *45*, 768−778.
(30) Tyagi, P.; Cooney, R. R.; Sewall, S. L.; Sagar, D. M.; Saari, J. I.; Kambhampati, P. Controlling Piezoelectric Response in Semiconductor Quantum Dots via Impulsive Charge Localization. *Nano Lett.* **2010**, *10*, 3062−3067.
(31) Krauss, T. D.; Wise, F. W. Coherent Acoustic Phonons in a Semiconductor Quantum Dot. *Phys. Rev. Lett.* **1997**, *79*, 5102−5105.
(32) Nisoli, M.; De Silvestri, S.; Cavalleri, A.; Malvezzi, A. M.; Stella, A.; Lanzani, G.; Cheyssac, P.; Kofman, R. Coherent Acoustic Oscillations in Metallic Nanoparticles Generated with Femtosecond Optical Pulses. *Phys. Rev. B* **1997**, *55*, 13424−13427.
(33) Hodak, J. H.; Martini, I.; Hartland, G. V. Observation of Acoustic Quantum Beats in Nanometer Sized Au Particles. *J. Chem. Phys.* **1998**, *108*, 9210−9213.
(34) Del Fatti, N.; Voisin, C.; Chevy, F.; Vallée, F.; Flytzanis, C. Coherent Acoustic Mode Oscillation and Damping in Silver Nanoparticles. *J. Chem. Phys.* **1999**, *110*, 11484−11487.
(35) Dubrovskiy, V. A.; Morochnik, V. S. Natural Vibrations of a Spherical Inhomogeneity in an Elastic Medium. *Earth Phys.* **1981**, *17*, 494−504.
(36) Hodak, J. H.; Henglein, A.; Hartland, G. V. Size Dependent Properties of Au Particles: Coherent Excitation and Dephasing of Acoustic Vibrational Modes. *J. Chem. Phys.* **1999**, *111*, 8613−8621.
(37) Juvé, V.; Crut, A.; Maioli, P.; Pellarin, M.; Broyer, M.; Del Fatti, N.; Vallée, F. Probing Elasticity at the Nanoscale: Terahertz Acoustic Vibration of Small Metal Nanoparticles. *Nano Lett.* **2010**, *10*, 1853−1858.
(38) Sauceda, H. E.; Mongin, D.; Maioli, P.; Crut, A.; Pellarin, M.; Del Fatti, N.; Vallée, F.; Garzón, I. L. Vibrational Properties of Metal Nanoparticles: Atomistic Simulation and Comparison with Time-Resolved Investigation. *J. Phys. Chem. C* **2012**, *116*, 25147−25156.
(39) Varnavski, O.; Ramakrishna, G.; Kim, J.; Lee, D.; Goodson, T. Optically Excited Acoustic Vibrations in Quantum-Sized Monolayer-Protected Gold Clusters. *ACS Nano* **2012**, *4*, 3406−3412.
(40) Qian, H. F.; Sfeir, M. Y.; Jin, R. C. Ultrafast Relaxation Dynamics of $[Au_{25}(SR)_{18}]^q$ Nanoclusters: Effects of Charge State. *J. Phys. Chem. C* **2010**, *114*, 19935−19940.
(41) Miller, S. A.; Womick, J. M.; Parker, J. F.; Murray, R. W.; Moran, A. M. Femtosecond Relaxation Dynamics of $Au_{25}L_{18}^-$ Monolayer-Protected Clusters. *J. Phys. Chem. C* **2009**, *113*, 9440−9444.
(42) Cerullo, G.; De Silvestri, S.; Banin, U. Size-Dependent Dynamics of Coherent Acoustic Phonons in Nanocrystal Quantum Dots. *Phys. Rev. B* **1999**, *60*, 1928−1932.
(43) Huxter, V. M.; Lee, A.; Lo, S. S.; Scholes, G. D. CdSe Nanoparticle Elasticity and Surface Energy. *Nano Lett.* **2009**, *9*, 405−409.
(44) Yu, K.; Zijlstra, P.; Sader, J. E.; Xu, Q.-H.; Orrit, M. Damping of Acoustic Vibrations of Immobilized Single Gold Nanorods in Different Environments. *Nano Lett.* **2013**, *13*, 2710−2716.
(45) Landau, L. D.; Lifshitz, E. M. *Theory of Elasticity*; Elsevier: Oxford, U.K., 1970; Vol. 7, pp 438−442.
(46) Love, A. E. H. *A Treatise on the Mathematical Theory of Elasticity*; Cambridge University Press: London, 1934.
(47) Crut, A.; Maioli, P.; Del Fatti, N.; Vallée, F. Anisotropy Effects on the Time-Resolved Spectroscopy of the Acoustic Vibrations of Nanoobjects. *Phys. Chem. Chem. Phys.* **2009**, *11*, 5882−5888.
(48) Zijlstra, P.; Tchebotareva, A. L.; Chon, J. W. M.; Gu, M.; Orrit, M. Acoustic Oscillations and Elastic Moduli of Single Gold Nanorods. *Nano Lett.* **2008**, *8*, 3493−3497.
(49) Hartland, G. V; Hu, M.; Wilson, O.; Mulvaney, P.; Sader, J. E. Coherent Excitation of Vibrational Modes in Gold Nanorods. *J. Phys. Chem. B* **2002**, *106*, 743−747.
(50) Hu, M.; Hillyard, P.; Hartland, G. V; Kosel, T.; Perez-Juste, J.; Mulvaney, P. Determination of the Elastic Constants of Gold Nanorods Produced by Seed Mediated Growth. *Nano Lett.* **2004**, *4*, 2493−2497.
(51) Petrova, H.; Perez-Juste, J.; Zhang, Z. Y.; Zhang, J.; Kosel, T.; Hartland, G. V. Crystal Structure Dependence of the Elastic Constants of Gold Nanorods. *J. Mater. Chem.* **2006**, *16*, 3957−3963.
(52) Sando, G. M.; Berry, A. D.; Owrutsky, J. C. Ultrafast Studies of Gold, Nickel, and Palladium Nanorods. *J. Chem. Phys.* **2007**, *127*, 074705.
(53) Pomfret, M. B.; Brown, D. J.; Epshteyn, A.; Purdy, A. P.; Owrutsky, J. C. Electrochemical Template Deposition of Aluminum Nanorods Using Ionic Liquids. *Chem. Mater.* **2008**, *20*, 5945−5947.
(54) Owrutsky, J. C.; Pomfret, M. B.; Brown, D. J. Coherent Acoustic Oscillations of Nanorods Composed of Various Metals. *J. Phys. Chem. C* **2009**, *113*, 10947−10955.
(55) Jerebtsov, S. N.; Kolomenskii, A. A.; Liu, H. D.; Zhang, H.; Ye, Z. X.; Luo, Z. P.; Wu, W. H.; Paulus, G. G.; Schuessler, H. A. Laser-

Excited Acoustic Oscillations in Silver and Bismuth Nanowires. *Phys. Rev. B* **2007**, *76*, 184301.
(56) Staleva, H.; Hartland, G. V. Vibrational Dynamics of Silver Nanocubes and Nanowires Studied by Single-Particle Transient Absorption Spectroscopy. *Adv. Funct. Mater.* **2008**, *18*, 3809−3817.
(57) Kolomenskii, A. A.; Jerebtsov, S. N.; Liu, H. D.; Zhang, H.; Ye, Z. X.; Luo, Z. P.; Wu, W. H.; Schuessler, H. A. Observation of Coherent Acoustic and Optical Phonons in Bismuth Nanowires by a Femtosecond Pump−Probe Technique. *J. Appl. Phys.* **2008**, *104*, 103110.
(58) Son, D. H.; Wittenberg, J. S.; Banin, U.; Alivisatos, A. P. Second Harmonic Generation and Confined Acoustic Phonons in Highly Excited Semiconductor Nanocrystals. *J. Phys. Chem. B* **2006**, *110*, 19884−19890.
(59) Lo, S. S.; Major, T. A.; Petchsang, N.; Huang, L. B.; Kuno, M. K.; Hartland, G. V. Charge Carrier Trapping and Acoustic Phonon Modes in Single CdTe Nanowires. *ACS Nano* **2012**, *6*, 5274−5282.
(60) Lohse, S. E.; Murphy, C. J. The Quest for Shape Control: A History of Gold Nanorod Synthesis. *Chem. Mater.* **2013**, *25*, 1250−1261.
(61) Staleva, H.; Skrabalak, S. E.; Carey, C. R.; Kosel, T.; Xia, Y. N.; Hartland, G. V. Coupling to Light, and Transport and Dissipation of Energy in Silver Nanowires. *Phys. Chem. Chem. Phys.* **2009**, *11*, 5889−5896.
(62) Hodak, J. H.; Henglein, A.; Hartland, G. V. Coherent Excitation of Acoustic Breathing Modes in Bimetallic Core−Shell Nanoparticles. *J. Phys. Chem. B* **2000**, *104*, 5053−5055.
(63) Sader, J. E.; Hartland, G. V; Mulvaney, P. Theory of Acoustic Breathing Modes of Core−Shell Nanoparticles. *J. Phys. Chem. B* **2002**, *106*, 1399−1402.
(64) Kirakosyan, A. S.; Shahbazyan, T. V. Vibrational Modes of Metal Nanoshells and Bimetallic Core−Shell Nanoparticles. *J. Chem. Phys.* **2008**, *129*, 034708.
(65) Guillon, C.; Langot, P.; Del Fatti, N.; Vallée, F.; Kirakosyan, A. S.; Shahbazyan, T. V; Cardinal, T.; Treguer, M. Coherent Acoustic Vibration of Metal Nanoshells. *Nano Lett.* **2007**, *7*, 138−142.
(66) Mongin, D.; Juvé, V.; Maioli, P.; Crut, A.; Del Fatti, N.; Vallée, F.; Sanchez-Iglesias, A.; Pastoriza-Santos, I.; Liz-Marzan, L. M. Acoustic Vibrations of Metal−Dielectric Core−Shell Nanoparticles. *Nano Lett.* **2011**, *11*, 3016−3021.
(67) Dowgiallo, A. M.; Knappenberger, K. L. Influence of Confined Fluids on Nanoparticle-to-Surroundings Energy Transfer. *J. Am. Chem. Soc.* **2012**, *134*, 19393−19400.
(68) Newhouse, R. J.; Wang, H. N.; Hensel, J. K.; Wheeler, D. A.; Zou, S. L.; Zhang, J. Z. Coherent Vibrational Oscillations of Hollow Gold Nanospheres. *J. Phys. Chem. Lett.* **2011**, *2*, 228−235.
(69) Hu, M.; Petrova, H.; Wang, X.; Hartland, G. V. Time-Resolved and Steady State Spectroscopy of Polydisperse Colloidal Silver Nanoparticle Samples. *J. Phys. Chem. B* **2005**, *109*, 14426−14432.
(70) Petrova, H.; Lin, C. H.; de Liejer, S.; Hu, M.; McLellan, J. M.; Siekkinen, A. R.; Wiley, B. J.; Marquez, M.; Xia, Y. N.; Sader, J. E.; et al. Time-Resolved Spectroscopy of Silver Nanocubes: Observation and Assignment of Coherently Excited Vibrational Modes. *J. Chem. Phys.* **2007**, *126*, 094709.
(71) Petrova, H.; Lin, C. H.; Hu, M.; Chen, J. Y.; Siekkinen, A. R.; Xia, Y. N.; Sader, J. E.; Hartland, G. V. Vibrational Response of Au−Ag Nanoboxes and Nanocages to Ultrafast Laser-Induced Heating. *Nano Lett.* **2007**, *7*, 1059−1063.
(72) Tchebotareva, A. L.; van Dijk, M. A.; Ruijgrok, P. V; Fokkema, V.; Hesselberth, M. H. S.; Lippitz, M.; Orrit, M. Acoustic and Optical Modes of Single Dumbbells of Gold Nanoparticles. *ChemPhysChem* **2009**, *10*, 111−114.
(73) Kelf, T. A.; Tanaka, Y.; Matsuda, O.; Larsson, E. M.; Sutherland, D. S.; Wright, O. B. Ultrafast Vibrations of Gold Nanorings. *Nano Lett.* **2011**, *11*, 3893−3898.
(74) Fedou, J.; Viarbitskaya, S.; Marty, R.; Sharma, J.; Paillard, V.; Dujardin, E.; Arbouet, A. From Patterned Optical Near-Fields to High Symmetry Acoustic Vibrations in Gold Crystalline Platelets. *Phys. Chem. Chem. Phys.* **2013**, *15*, 4205−4213.
(75) Major, T. A.; Devadas, M. S.; Lo, S. S.; Hartland, G. V. Optical and Dynamical Properties of Chemically Synthesized Gold Nanoplates. *J. Phys. Chem. C* **2013**, *117*, 1447−1452.
(76) Crut, A.; Juvé, V.; Mongin, D.; Maioli, P.; Del Fatti, N.; Vallée, F. Vibrations of Spherical Core−Shell Nanoparticles. *Phys. Rev. B* **2011**, *83*, 9.
(77) Johnson, C. J.; Dujardin, E.; Davis, S. A.; Murphy, C. J.; Mann, S. Growth and Form of Gold Nanorods Prepared by Seed-Mediated, Surfactant-Directed Synthesis. *J. Mater. Chem.* **2002**, *12*, 1765−1770.
(78) Belliard, L.; Cornelius, T. W.; Perrin, B.; Kacemi, N.; Becerra, L.; Thomas, O.; Toimil-Molares, M. E.; Cassinelli, M. Vibrational Response of Free Standing Single Copper Nanowire through Transient Reflectivity Microscopy. *J. Appl. Phys.* **2013**, *114*, 193509.
(79) Staleva, H.; Hartland, G. V. Transient Absorption Studies of Single Silver Nanocubes. *J. Phys. Chem. C* **2008**, *112*, 7535−7539.
(80) Burgin, J.; Langot, P.; Del Fatti, N.; Vallée, F.; Huang, W.; El-Sayed, M. A. Time-Resolved Investigation of the Acoustic Vibration of a Single Gold Nanoprism Pair. *J. Phys. Chem. C* **2008**, *112*, 11231−11235.
(81) Saviot, L.; Netting, C. H.; Murray, D. B. Damping by Bulk and Shear Viscosity of Confined Acoustic Phonons for Nanostructures in Aqueous Solution. *J. Phys. Chem. B* **2007**, *111*, 7457−7461.
(82) Liu, M. Z.; Guyot-Sionnest, P. Mechanism of Silver(I)-Assisted Growth of Gold Nanorods and Bipyramids. *J. Phys. Chem. B* **2005**, *109*, 22192−22200.
(83) Hartland, G. V. Ultrafast Studies of Single Semiconductor and Metal Nanostructures through Transient Absorption Microscopy. *Chem. Sci.* **2010**, *1*, 303−309.